Space-charge-induced acceleration of ions emitted by laser-irradiated surfaces

A. J. Peurrung, J. P. Cowin, G. Teeter,[a] S. E. Barlow, and T. M. Orlando[b]
Molecular Science Research Center, Pacific Northwest Laboratory, Richland, Washington 99352

(Received 2 March 1994; accepted for publication 5 March 1995)

Pulsed-laser-irradiated surfaces sometimes emit positive ions at energies several volts higher than one would expect, even at modest (<0.1 J/cm^2) fluences. A mechanism that can account for this phenomenon is discussed. Intense surface photoemission of electrons during the laser pulse leads to the formation of a space-charge layer near the surface. If the laser fluence were constant, the ions would accelerate and subsequently decelerate as they pass through this steady potential well. As the laser pulse ends, however, some ions may undergo extended acceleration as this space-charge layer moves away from the surface. The maximum possible ion acceleration is analytically calculated and the acceleration for a range of realistic experimental parameters is numerically predicted. © *1995 American Institute of Physics.*

I. INTRODUCTION

It is very common to utilize high-powered pulsed (ns) lasers in desorption,[1-3] surface photochemistry,[4-7] and material ablation[8-10] studies. The fluences (0.001 J/cm^2$<f<$10.0 J/cm^2) typically used in these experiments vary over several orders of magnitude and the effects range from perturbative to destructive. The laser-surface interaction progresses from thermal heating to neutral desorption and ultimately to explosive ablation and plasma plume production as the fluence increases. The plasma plume threshold is generally at fluences greater than about 1 J/cm^2 (1 GW/cm^2 for a 2 ns pulse); in this regime the observed outgoing products result from a complex variety of electronic and chemical processes in the ablation plume.[10] Laser-induced emission of positive ions with kinetic energies much greater than thermal has been reported[11-13] in laser-surface experiments which have been carried out under seemingly mild irradiation conditions ($\leq$0.1 J/cm^2). Although these fluences are well below the plasma plume production threshold, the ion yield and energy distributions[12] indicate the possibility of ion acceleration via collective effects in the electron space-charge cloud produced via photoemission.[14] This type of dynamical acceleration was suggested as a mechanism for the laser-induced emission of translationally hot ($\approx$0.7 eV) positive ions from Cu(100) at a power threshold of $\approx$60 MW/cm^2.[12] Note that the acceleration mechanism discussed in this article applies only in the low-fluence regime where the ion yield can be regarded as exceedingly small. For example, the model works well for ion yields of approximately 10^2–10^4 per laser shot. When the ion yield becomes substantially greater, the "Coulomb explosion" model[11] is generally more applicable.

Previous study of particle acceleration by time-dependent space-charge fields in the low-fluence limit has been restricted to electrons.[15,16] It has been shown[15] that the earliest emitted electrons gain 3–4.5 eV as a rapidly forming negative space-charge potential layer accelerates away from the surface when the laser pulse turns on. Acceleration only occurs for those electrons that escape before the formation of a primary, negative space-charge layer. Acceleration in this case is a rapid, transient phenomenon; on the time scale for electron acceleration the laser pulse and its associated space-charge layer are approximately constant. Ion acceleration occurs by a very different process since the mechanism for electron acceleration is too rapid for effective ion acceleration. Instead, ion acceleration is caused by the primary space-charge layer as it moves slowly away from the surface when the laser pulse decays. Thus, an ion emitted from the surface, or created in the near-surface zone at a suitable time and with an appropriate initial kinetic energy, may experience a substantial energy gain if it is able to move along with the accelerating space-charge layer.[14] This article presents an analytical description of space-charge-induced acceleration of ions in a fluence region that has received little attention, i.e., near the plasma threshold region. We provide numerical results that cover a range of experimentally relevant parameters. Section II reviews the known structure of the space-charge layer and places upper and lower bounds on the laser fluence for which our treatment can be considered valid. Section III details the main results concerning ion acceleration and derives an analytical expression for the maximum energy gain that is theoretically possible. Section IV tests the validity of our simple dynamical analysis of ion motion by carefully examining a number of assumptions inherent in the model.

II. SPACE-CHARGE MODEL

The effect of space charge on the ability of a planar vacuum gap to carry a current has previously been studied since it is related to the performance of vacuum tubes.[17] These calculations show that the maximum transmittable current J_t across a gap of width L by electrons with charge $-e$, mass m_e, and initial energy E_0 is

$$J_t=\frac{4\epsilon_0}{9}\left(\frac{2e}{m_e}\right)^{1/2}\frac{E_0^{3/2}}{L^2}. \quad (1)$$

[a]Present address: Department of Physics, University of Texas at Austin, Austin, TX 76712.
[b]Author to whom correspondence should be addressed.

 0021-8979/95/78(1)/481/8/$6.00

For typical parameters such as $E_0=1.0$ eV and $L=0.1$ cm, Eq. (1) predicts a maximum current density of 230 μA/cm^2 or roughly six orders of magnitude less than the 100 A/cm^2 photoelectron current density that is typically emitted from a surface during a laser pulse.[15] The vast majority of the emitted current returns to the emitting surface because of repulsion from the existing negative space charge and attraction to the positive, image space charge inside the emitting material (which we assume is conductive). Equation (1) is the well known Child–Langmuir law of space-charge-limited current in a planar diode.[17]

The potential ϕ as a function of the coordinate z, which measures distance from the emitting surface, is the unique, self-consistent solution to the Poisson equation $[\nabla^2\phi(z)=-ne/\epsilon_0]$ and the Lorentz force equation $[m_e(d^2z/dt^2)=-e(d\phi/dz)]$ that satisfies the appropriate boundary conditions for electron motion. It is necessary for us to make some assumption regarding the distribution of photoelectron emission energies. Electron photoemission tends to occur with energy distributions that mirror the occupied states within the emitting surface. For a metallic source as assumed here, the filled states tend to occur in a continuous band. Thus, if we assume that the energies of the emitted electrons are uniformly distributed between 0 and E_0, then the transmitted current is closely approximated by Eq. (1) as long as $J_t \ll J_0$, where J_0 is the current density emitted from the surface. This "step-function" electron energy distribution is used throughout this article as a reasonable model for the energy distribution observed in experiments. In this case the potential across the gap becomes

$$\phi(z)=\begin{cases} \dfrac{-E_0}{e}\left(1-\dfrac{(z_0-z)^4}{z_0^4}\right), & 0\leqslant z\leqslant z_0, \\ \dfrac{-E_0}{e}\left[1-\left(\dfrac{z-z_0}{L-z_0}\right)^{4/3}\right], & z_0\leqslant z\leqslant L, \end{cases} \tag{2}$$

where the emitting surface is at $z=0$. Note that the effect of image charges within the metallic emitting surface is automatically contained in Eq. (2). The parameter z_0 is the location where the minimum in the space-charge potential occurs,

$$z_0=\left(\frac{18\epsilon_0^2}{e^2m_e}\right)^{1/4}\frac{E_0^{3/4}}{J_0^{1/2}}, \tag{3}$$

and it follows from our previous assumptions that $z_0 \ll L$. Figure 1 shows the space-charge-induced potential throughout the current-carrying vacuum gap. Notice that the potential is zero at both the emitting surface and the collector, but reaches a minimum at $z=z_0$ very near the emitting surface. For typical parameters ($J_0=100$ A/cm^2, $z_0/L=0.004$), the depth of the potential well is such that it is able to reflect the vast majority of photoemitted electrons; i.e., $\phi(z_0)=E_0/e$.

The above solution for $\phi(z)$ and z_0 is valid only for a restricted range of J_0. Although we expect that the low-fluence regime considered in this work should be restricted to $f<1$ J/cm^2, it is important to consider established upper bounds to the laser fluence for which Eq. (2) and (3) can be

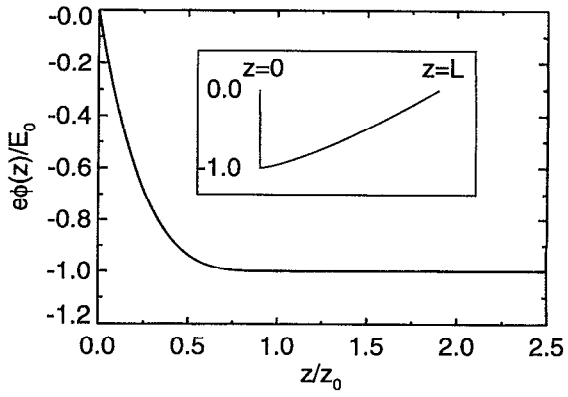

FIG. 1. One-dimensional space-charge potential ϕ vs gap coordinate z. The potential across the entire gap is shown in the inset. This model assumes that $J_t \ll J_0$ and $z_0 \ll L$. The typical values assumed in this article are $z_0=4\times10^{-4}$ cm and $E_0=1.0$ eV.

considered valid. An inverse bremsstrahlung-heated ion-electron plasma dominates the laser-surface interaction whenever[18,19]

$$P\sqrt{\tau}\geqslant C, \tag{4}$$

where P is the incident laser power, τ is the beam duration, and $C=2\times10^5$ W$\sqrt{\text{s}}$/cm^2 is an empirical constant appropriate for $\tau<10$ ns.[20] Whenever the laser fluence is this large, the resulting gross plasma plume makes our space-charge processes irrelevant. Our space-charge model could hold only in the low-laser-fluence limit where Eq. (4) is not satisfied ($P<2\times10^9$ W/cm^2 for $\tau=10$ ns). Assuming a quantum efficiency of 10^{-3} for electron photoemission and photon energies of 6 eV, Eq. (4) restricts the photoemitted electron current to $J_0<300$ kA/cm^2 for 10 ns pulses or a maximum laser fluence of 20 J/cm^2.

Another upper bound for J_0 is implicit in our assumption that the space-charge layer can be treated as a continuous electron "fluid." This condition can be expressed numerically by requiring that an accelerating ion interacts with a large number of separate electrons. Equation (2) and the Poisson equation combine to yield the electron number density n in the space-charge layer,

$$n(z)=\frac{4J_0}{e}\left(\frac{m_e}{2E_0}\right)^{1/2}\left(\frac{z_0-z}{z_0}\right)^2. \tag{5}$$

Integrating Eq. (5) from $z=0$ to $z=z_0$ gives the number density per unit surface area $\sigma=(z_0/3)n(0)$, and thus the total number of electrons in a cube with side length z_0 is $N=z_0^3n(0)/3$. Assuming $E_0=1.0$ eV, we find that $N<1$ when $J_0>10^6$ A/cm^2. Collective dynamics occurs whenever $N\gg1$, or equivalently, $f\ll60$ J/cm^2. As stated in Sec. I, the low-fluence regime considered here is restricted to $f<1$ J/cm^2. It follows that both of the above limits to laser fluence are readily satisfied.

A lower bound on J_0 arises from our assumption that $J_t \ll J_0$. At very low laser fluences, the photoemitted electron current may become comparable to the maximum current that can be transmitted across the gap according to the Child–Langmuir law. Specifically, Eqs. (2) and (3) are not

accurate when J_t is not much less than $J_r(z)$, where $J_r(z)$ is the current at location z that ultimately is reflected by the space-charge layer. Since we have assumed that the electrons have a uniform distribution of initial kinetic energies, the reflected current can be written

$$J_r(z)=J_0\left(\frac{z_0-z}{z_0}\right)^4. \tag{6}$$

From this equation we conclude that our space-charge equations are not accurate for the region where

$$\frac{z-z_0}{z_0}<\left(\frac{J_t}{J_0}\right)^{1/4}. \tag{7}$$

For $E_0=1.0$ eV and $J_0=100$ A/cm^2, the equations are accurate for all but a small region near $z=z_0^0$. Only when the photoemitted current has dropped to $J_0\approx 4\times 10^{-3}$ A/cm^2 does the analytic solution for the gap potential lose validity over a region in z as wide as $0.5z_0$. This problem is not even as severe as it may appear since relatively little ion acceleration occurs in the region around $z=z_0$. Nevertheless, for extremely low laser fluences this model is only approximate. The assumption that $z_0\ll L$ can also be violated for very low emitted currents. For example, when $J_0\approx 4\times 10^{-3}$ A/cm^2 and $E_0=1.0$ eV, the minimum in the potential occurs at $z_0=0.1$ cm.

III. ION ACCELERATION

The net energy gained by many emitted ions arises from their interaction with a time-dependent electron space-charge layer. If the space-charge potential were unchanging, positive ions would accelerate in the region $0<z<z_0$ but decelerate in the region $z_0<z<L$ thereby arriving at the collector with precisely their initial kinetic energy. A permanent energy gain by the ions occurs during the time when the laser fluence decreases. The space-charge potential well into which the ions are attracted moves away from the surface at this time because $z_0\propto J_0^{-1/2}$. By the time a particular ion reaches the location where it would have decelerated, the space-charge potential has moved so that the ion retains its acquired velocity and possibly even continues to accelerate. In many circumstances ions never decelerate because they never catch up to the minimum in the potential well. In essence, ions interact with the time-dependent space-charge potential much as an ocean surfer interacts with a surface water wave. Implicit in this model is the assumption that ion acceleration is a sufficiently slow process that the potential created by the emitted electrons moves "adiabatically," always retaining its steady-state form. The validity of this assumption is examined in Sec. IV.

The surprisingly strong acceleration undergone by some ions (>2.0 eV energy gain can occur even when the maximum emitted electron energy E_0 is 1.0 eV) is primarily a result of the detailed form of the space-charge potential well. The electric field that accelerates the ions is

$$-\frac{\partial\phi}{\partial z}=\frac{4E_0}{ez_0}\left(\frac{z_0-z}{z_0}\right)^3, \quad z<z_0. \tag{8}$$

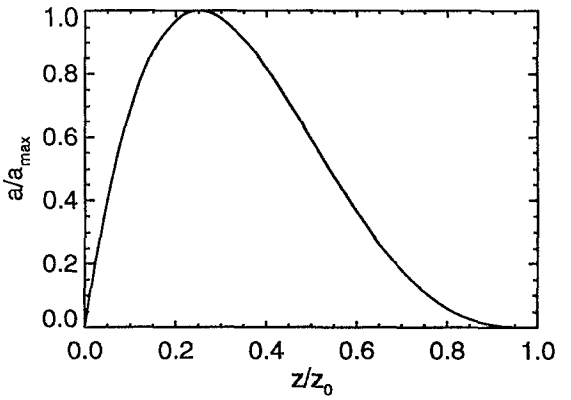

FIG. 2. Ion acceleration a vs the location z_0 of the minimum in the space-charge potential. The ion's position z is fixed. The acceleration is normalized to the maximum possible acceleration at $z_0=4z$. Substantial acceleration occurs over a large range in z_0.

For arbitrary laser time profiles [i.e., $z_0(t)$ profiles], ion emission times, and initial kinetic energies, we can numerically integrate Eq. (8) to find the total work performed on the ion by the space-charge electric field. Before discussing this general case in detail, however, it is useful to know the theoretical maximum possible energy gain. For an ion located at position z, there is a particular laser fluence that maximizes the force on that ion. Figure 2 shows the acceleration for an ion at z as a function of z_0 (which depends on the instantaneous laser fluence). An accelerating ion for which we continuously adjust the laser fluence in order to maintain this maximum force should therefore receive the maximum possible energy gain. The maximum electric field for an ion as a fixed position z occurs when $z_0=4z$ and leads to an acceleration

$$a_{\max}=\left(\frac{3}{4}\right)^3\frac{E_0}{m_i z}. \tag{9}$$

The theoretical maximum possible work that may be performed on the ion is obtained by requiring the laser's time profile to be such that $z_0=4z$ at all times. In this way we guarantee that Eq. (9) describes the ion acceleration for all possible values of z.

The total amount of work performed on an accelerating ion under "optimal" conditions is given by

$$\Delta U_{\mathrm{KE}}=U_{\mathrm{KE}}(z_s)-U_{\mathrm{KE}}(0)+\int_{z_s}^{z_f}(m_i a_{\max})dz, \tag{10}$$

where $z=0$ is the emitting surface and maximum acceleration occurs between $z=z_s$ and $z=z_f$. Maximum acceleration is not possible all of the way from $z=0$ because this would require an infinite laser fluence. We assume that maximum acceleration begins at $z_s=z_0^0/4$, where z_0^0 is the location of the space-charge potential minimum at peak photoelectron current J_0. The acceleration trajectory is assumed to stop at $z_f=L/2$, where L is the width of the vacuum gap. Using Eqs. (2) and (9), Eq. (10) can be rewritten

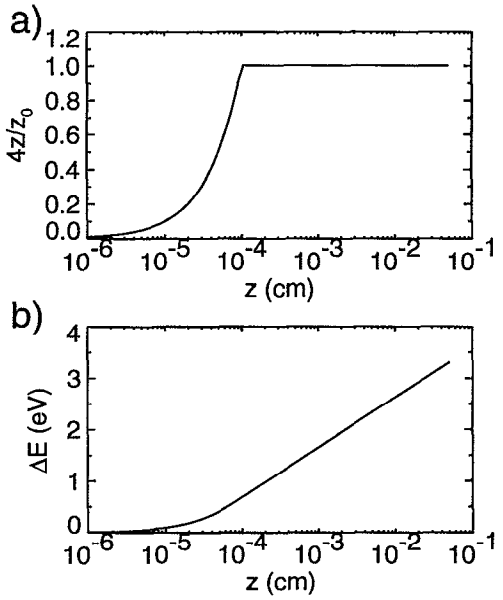

FIG. 3. Ion position relative to (a) the space-charge potential minimum and (b) the energy gain vs position for an optimal acceleration trajectory. After reaching $z=1.0\times10^{-4}$ cm, the ion remains perfectly positioned for maximum acceleration and energy gain depends logarithmically on distance traveled. The peak photoelectron current is $J_0=100$ A/cm^2 and the peak photoelectron energy is $E_0=1.0$ eV.

$$\Delta U_{\mathrm{KE}}=\left[1-\left(\frac{3}{4}\right)^4+\left(\frac{3}{4}\right)^3\ln\frac{2L}{z_0^0}\right]E_0. \tag{11}$$

Figure 3 characterizes the optimal ion acceleration when $J_0=100$ A/cm^2, $E_0=1.0$ eV, and $L=0.1$ cm. Figure 3(a) shows the ratio $4z/z_0$ during the entire trajectory. Until the ion reaches the location $z=z_0^0/4$, the laser fluence is constant and the potential well is steady. When $z>z_0^0/4$, however, the laser fluence must change to preserve maximum acceleration. Figure 3(b) shows $\Delta U_{\mathrm{KE}}(z)$ for the same ion and laser parameters used above. For the specific parameters used in Fig. 3, the ion's energy gain is $3.3E_0$. The numerically calculated laser profile that leads to maximum ion acceleration in this case is shown graphically in Fig. 4. Notice that for $z>z_0^0/4$, the ion gains energy logarithmically with distance traveled; each decade of distance that the ion travels brings the same energy gain. Based on Eq. (11) we also expect that the energy gain of an ion is relatively insensitive to parameters such as gap width L and peak photoelectron current J_0.

Equation (10) predicts the energy gain experienced by an ion as the laser fluence decreases to zero in a way that is optimized for maximum ion acceleration. It is also of interest to know the maximum ion acceleration that can be produced when a steady laser beam has a superimposed noise component. This case is substantially different because the laser fluence does not reach zero, but rather returns to a steady-state value. We assume that the laser normally causes the emission of a steady photoelectron current J_n but that the current momentarily rises to J_s during a spike in the laser fluence. The case where the laser output momentarily drops can be handled in a very similar fashion provided that the laser fluence does not drop too near to zero. As with the

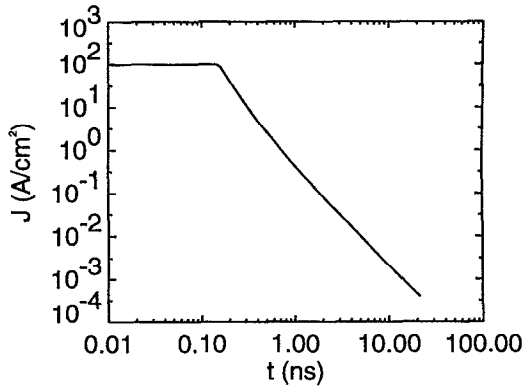

FIG. 4. Numerically calculated photocurrent vs time for maximum ion acceleration. The laser fluence decreases only after the ion reaches $z=4\times10^{-4}$ cm. This example is for an ion with mass $m_i=1$ u and peak photocurrent $J_0=100$ A/cm^2. The ion is emitted at $t=0$.

previous calculation of the ideal laser pulse profile, this calculation makes certain "worst-case" assumptions about a noise spike. For example, the rising edge of an upward-going spike is arbitrary, but the falling edge profile is assumed to lead to the maximum energy gain. Because the laser fluence in this case in not permanently decaying, the ion must decelerate after it passes through the minimum in the potential well. As an approximation, we assume that the acceleration of the ion into and out of the space-charge potential well ultimately cancel. Evaluating Eq. (10) with boundaries of integration representing the beginning and the end of the spike-induced acceleration yields the maximum energy gain from a single noise spike,

$$\Delta U_{\mathrm{KE}}=\left(\frac{27}{128}\ln\frac{J_s}{J_n}\right)E_0. \tag{12}$$

A noise spike in which the laser output momentarily doubles can produce an ion energy gain of no more than $0.15E_0$. This is true only for spikes on time scales greater than roughly 100 ps; the energy gain from shorter spikes is substantially less. This type of acceleration is therefore generally unimportant.

A number of different parameters must be taken into account when characterizing the acceleration of an entire population of ions emitted during a typical pulsed laser surface experiment. The laser profiles used in actual experiments are quite unlike the ideal profiles that produce the maximum ion acceleration, but a surprisingly large amount of acceleration can still take place. We use two different laser profiles in our numerical study of ion acceleration. The Gaussian profile, $J(t)=J_0\exp(-t^2/\tau_0^2)$, approximates the output of common, commercially available lasers except when $|t/\tau_0|\gg1$, where most laser profiles are not well specified. The simple analytic profile that produces a large acceleration is the "t^{-4}" profile, $J(t)=J_0/[1+(t/\tau_0)^4]$. For both cases the decay time τ_0 is typically chosen to be 1.0 ns. Assuming that the laser pulse profile is well known, the most important remaining parameters are the ion's launch time t_l, initial kinetic energy E_i, and mass m_i. The launch time is measured relative to the time at which the laser pulse

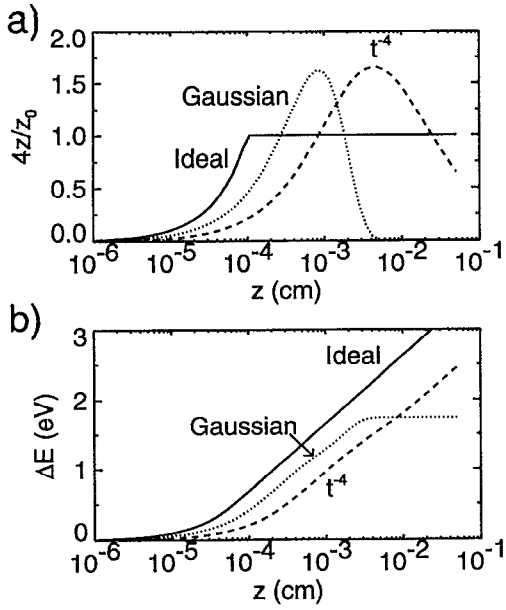

FIG. 5. Relative (a) location and (b) energy of an accelerating ion as it traverses the gap. Gaussian, t^{-4}, and idealized laser pulse profiles are used. The optimal launch times for Gaussian and t^{-4} laser profiles are 1.05 and 1.88 ns, respectively. Total energy gain depends largely on how the ion is positioned relative to the space-charge potential minimum as it traverses the gap.

reaches peak intensity. Negative launch times correspond to ions launched before the peak of the laser pulse, whereas positive launch times are after the peak. Unless otherwise stated, the initial kinetic energy is 0 eV and the ion mass is 1 u. We also assume that the maximum photoelectron energy is 1.0 eV and that the gap length is 0.1 cm.

Figure 5 characterizes the ion acceleration for the Gaussian, t^{-4}, and the "ideal" laser pulse shapes and helps to explain why substantial acceleration occurs in these cases. The particular trajectories shown are optimal, that is, the launch time is such that overall energy gain is maximized. Figure 5(a) shows the ion's position relative to the minimum in the space-charge potential as the ion crosses the gap. Remember that when $4z/z_0=1.0$ the ion's acceleration is maximized. (This is true for $z>z_0^0/4$ in the ideal case, which is shown for comparison.) The horizontal axis in this figure is logarithmic since under optimal conditions each decade of gap distance contributes equally to energy gain. From Fig. 5(a) we expect that a t^{-4} laser profile should lead to a large energy gain since the ion's acceleration is nearly optimal over a large range in z. Figure 5(b) shows the ion's energy profiles as they cross the gap. The Gaussian laser pulse decays so rapidly that the ion largely stops accelerating after it has crossed only 3% of the gap. Even with this limitation, this ion gains more than 1.7 times the maximum photoelectron energy as a result of the time dependence of the space-charge potential well.

An ion's energy gain is moderately sensitive to its launch time. The launch time determines how effectively a particular ion is able to "surf" the moving space-charge potential. Figure 6 shows the energy gain as a function of distance for three ions launched early, optimally, and late ($t_l=0$, 1.88,

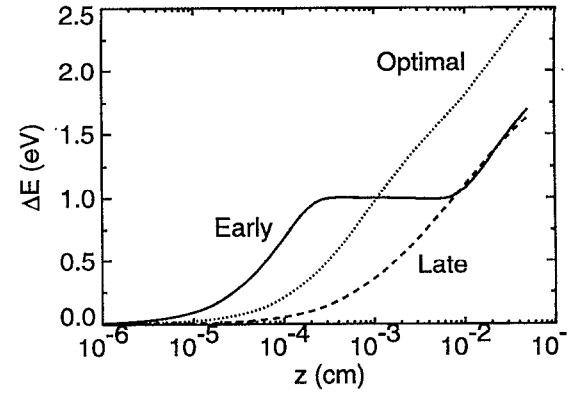

FIG. 6. Energy gain pattern for an ion launched early (0.0 ns), optimally (1.88 ns), and late (3.76 ns) during a laser pulse with a t^{-4} temporal profile.

and 3.76 ns) with a t^{-4} laser pulse profile. The early ion accelerates strongly for a while but eventually gets ahead of the space-charge layer and must wait for the potential well to "catch up." The optimally launched ion accelerates approximately evenly across the entire gap (once it has reached the starting point at $z_0^0/4$). The late ion experiences weak acceleration near the surface and therefore gains less energy. Figure 7 shows the energy gain as a function of launch time for both Gaussian and t^{-4} laser profiles. In both cases ions are strongly accelerated for a wide range of launch times that are coincident with the laser pulse. Little acceleration is felt only for ions launched more than 2.0 ns after the peak of a Gaussian laser pulse. Note that maximum acceleration always occurs for ions launched during the trailing edge of the laser pulse; this is a physically realistic launch time since the ions observed by Strupp and co-workers[12] are believed to be produced by electron collisions with thermally desorbed atoms. Though the mass of the ion was not identified in this reference, it is interesting to note that the experimentally observed positive ion kinetic energy distribution is qualitatively similar to the energy gain for H^+ calculated with a Gaussian laser pulse.

The initial ion kinetic energy has relatively little effect on its subsequent acceleration assuming that for each initial energy we choose the launch time that maximizes energy gain. Figure 8 shows the numerically calculated optimal en-

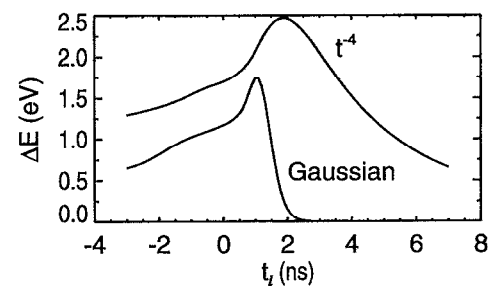

FIG. 7. Energy gain vs launch time for both Gaussian and t^{-4} laser pulse profiles. Note that maximum acceleration occurs for ions launched during the trailing edge of the laser pulse.

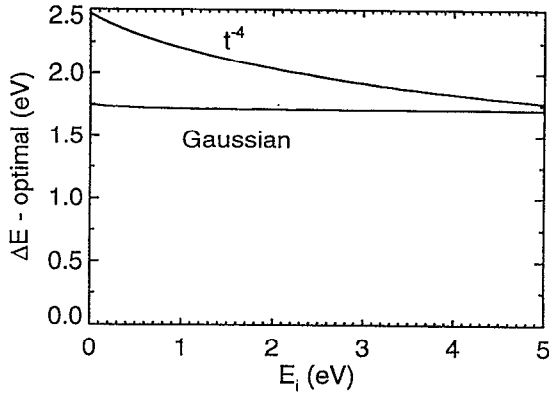

FIG. 8. Optimal energy gain vs initial kinetic energy. The launch time is chosen to maximize acceleration. Note that the ion acceleration is not very sensitive to the initial kinetic energy.

ergy gain for both Gaussian and t^{-4} profiles as a function of initial energy. The optimal launch time does depend slightly on initial ion energy. For example, with a Gaussian laser profile the optimal launch time is 1.05 ns when $E_i=0$ eV and 1.59 ns when $E_i=4.0$ eV. Generally, ions with larger initial energies have later optimal launch times. The surface plots in Fig. 9 show the energy gain over the entire experimentally accessible range of E_i and t_l. Note that the net acceleration for a Gaussian laser profile is remarkably independent of initial ion energy. From this figure one can again see that ion acceleration is a phenomenon that should affect a substantial fraction of the emitted ions.

The last parameter of experimental interest is ion mass. Although we have presented data exclusively for hydrogen ions (protons), the behavior is quite similar for ions of other masses. Figure 10 shows the optimal energy gain with both

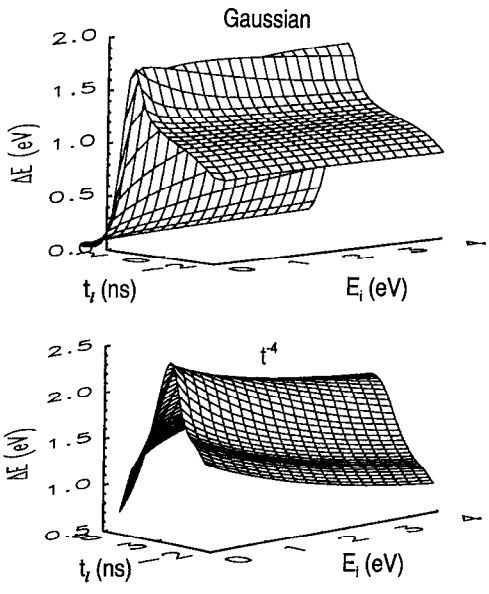

FIG. 9. Energy gain vs launch time and initial kinetic energy for both Gaussian and t^{-4} laser profiles. These contour profiles show the wide range of conditions for which substantial acceleration can occur.

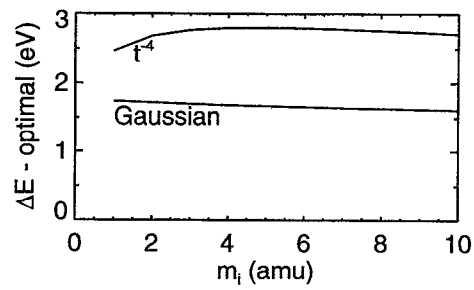

FIG. 10. Optimal energy gain vs ion mass for both Gaussian and t^{-4} laser profiles. The launch time is chosen to maximize acceleration. Note that the optimal energy gain is not very sensitive to the ion mass.

laser profiles as a function of ion mass. The detailed shape of these curves certainly depends on our choice of 1.0 ns for the laser pulse decay time τ_0, but the general trend is clear. Ion acceleration does not depend strongly on ion mass. The maximum acceleration occurs for the t^{-4} profile at a mass of $m_i=5$ u. The energy gain for this ion is 84% of the theoretical maximum acceleration of 3.3 eV. Of course, the optimal launch time also depends on ion mass. With a t^{-4} laser profile, for example, the optimal launch time is $t_l=1.88$ ns when $m_i=1$ u but 0.45 ns when $m_i=5$ u. Since maximum ion emission presumably occurs at peak laser fluence ($t_l=0$ ns), a population of D_2^+ ions ($m_i=4$ u) would therefore experience a larger average energy gain than a population of D^+ ions ($m_i=2$ u).

IV. NONIDEAL EFFECTS

There are several assumptions inherent in our numerical computation of the ion's interaction with the electron space-charge layer. Do the properties of the electron space-charge layer depend only on the value of the electron photocurrent $J(t)$ and not, for example, on its rate of change? We treat the electron space charge as a continuous fluid, rather than the nonneutral plasma that is really is. Are there any interactions that arise in a plasma that affect our conclusions? Does the passage of ions modify the space-charge layer in some way? This section attempts to answer these questions and test the validity of our assumptions.

The model for the electron space-charge layer discussed in Sec. II is a steady-state approximation. In order to determine whether this approximation can be used to analyze ion acceleration, the rate at which the space-charge layer reaches equilibrium τ_e must be compared to the time scale for changes of the laser fluence τ_f. We expect our equilibrium space-charge model to be applicable whenever $\tau_e<\tau_f$. The relaxation time for processes within the emitting surface (i.e., the image charge formation time) is assumed to be much smaller than τ_f. Since the space-charge layer constitutes a non-neutral plasma,[21] the equilibration time should be of the order of the period for plasma oscillations,[22] $\tau_e=2\pi/\omega_e$, where $\omega_e=(n_e e^2/\epsilon_0 m_e)^{1/2}$ is the plasma oscillation frequency and n_e is the electron density at the emitting surface. Gilton *et al.*[15] have numerically calculated the relaxation time for a space-charge layer formed by 100 A/cm^2 of emitted electron current where all electrons start with 1.0 eV of

energy. Their results indicate that the space-charge layer is fully formed 20 ps after the sudden onset of a laser pulse. Of course, τ_e increases as the laser fluence drops. Since the "plasma" density n_e is proportional to the emission current J_0, Eq. (3) implies that $\tau_e \propto z_0$. When the laser fluence has dropped so low that the space-charge layer is near the collector ($z_0 \approx L$), the relaxation time rises to $\tau_e \approx 5$ ns. The time scale $\tau_f = J(t)/(\partial J/\partial t)$ for changes in the laser fluence is easily calculated for both t^{-4} and Gaussian profiles. The result is

$$\textit{Gaussian:} \quad \tau_f = \frac{\tau_0^2}{2t} \tag{13}$$

$$t^{-4}: \quad \tau_f = \frac{\tau_0}{4}\left(\frac{1+(t/\tau_0)^4}{(t/\tau_0)^3}\right). \tag{14}$$

A careful comparison of τ_e and τ_f reveals that for both laser profiles $\tau_e < \tau_f$ fails to be true near the end of the ion trajectory. For the t^{-4} laser profile, $\tau_e \approx \tau_f$ when $z_0 = 0.1$ cm. Since this is the point at which the ion reaches the collector, we expect that our steady-state approximation remains valid. For the Gaussian laser profile, $\tau_e < \tau_f$ fails to be true for $t > 3\tau_0$; however, as shown in Fig. 5, ion acceleration has largely stopped by this time.

The two types of interaction between an ion and the electron space-charge layer are collective interactions and random, collisional interactions. Until this point we have implicitly neglected the random, collisional interaction between ions and electrons and instead focused on the ion's interaction with the space-charge potential collectively set up by the electrons. We now argue for the validity of this assumption. In practice, the ion emission rate is sufficiently small that ion-ion interactions can be ignored. Because this article is not concerned with the mechanisms for ion emission from surfaces, we also neglect the potentially strong interaction between an ion and its own image charge when they are near the emitting surface. In addition, the ion is regarded as a free particle; the recombination rate at these low densities is very slow. If a recombination event were to occur, the resulting neutral particle would obviously suffer no further acceleration, but would carry the previous momentum of the ion.

It is very difficult for electrons in a plasma to change the velocity of ions via collisions. For this reason, the effective ion-electron collision frequency ν_{ie} is slower by a factor of m_e/m_i than the corresponding electron-electron collision frequency,[23]

$$\nu_{ee} \approx \frac{8\pi n_e e^4 \ln \Lambda}{m_e^2 v_e^3}, \tag{15}$$

where v_e is the electron thermal velocity and $\ln \Lambda$ is approximately 3. A collision is defined as an event that changes the average electron's velocity vector by 90°. The application of Eq. (15) is only approximate since the plasma in the space-charge layer is far from thermal equilibrium. The ion-electron collision frequency for this system is $\nu_{ie} \approx 5 \times 10^5$ s^{-1}, where the electron density at the emitting surface is used and we assume that $J_0 = 100$ A/cm^2 and $m_i = 1$ u. Since the ion crosses the space-charge layer in approximately 10^{-10} s and reaches the collector in approximately 10^{-7} s, direct Coulomb collisions have a negligible effect on ion motion. Equivalently, the ordinary frictional drag force felt by the ion as it moves through the electron "fluid" is unimportant. A second, more subtle interaction may take place between the accelerating ion and the non-neutral electron "plasma" that makes up the space-charge layer. The passing ion attracts the electrons and must therefore perturb the form of the space-charge potential. For a stationary ion this effect is simply the well-known Debye shielding of particles within a plasma. The shielding electron cloud forms slightly behind a moving ion since a moving ion's position changes in the time required for the electrons to react.[24] The electric field from this electron cloud acts continuously on the ion and may act to slow it. In order to place an upper bound on the strength of this effect, we assume that the ion moves through the space-charge layer at the electron thermal speed. This assumption should greatly overestimate the strength of this effect since the ion actually moves much more slowly through the electron plasma. When moving at this speed, the ion's shielding cloud has a charge e and should form a distance λ_D behind the ion where $\lambda_D = [\epsilon_0 m_e v_e^2/2n(0)e^2]^{1/2}$ is the plasma's Debye length. When $J_0 = 100$ A/cm^2, the electric field from the shielding cloud at the ion's location is $E = e/\lambda_D^2 = 15$ V/cm, or roughly 1000 times less than the surface electric field assumed by the model. At lower laser fluences this disparity is even larger. We conclude, therefore, that this effect should not complicate the process of ion acceleration.

V. CONCLUSIONS

Even at low intensity, pulsed laser irradiation of a surface leads to the formation of a time-dependent electron space-charge layer that strongly effects the dynamics of emitted positive ions. Ions gain energy as they accelerate away from the surface with the space-charge layer during the trailing edge of the laser pulse. Theoretically, the maximum possible energy gain is proportional to the maximum photoelectron energy and to the logarithm of the acceleration distance. A simple yet accurate model can be used to study ion acceleration for a particular experimental situation. The energy gain experienced by a particular ion depends on many parameters such as the ion's mass, launch time, and initial kinetic energy. The detailed form of the laser pulse profile is also important in determining ion acceleration. For the Gaussian pulse profile with gap length 0.1 cm and a maximum photoelectron energy of 1.0 eV, hydrogen ions gain approximately 1.0 eV on average, while some ions may gain as much as 1.75 eV. Some ions accelerated by a longer-lasting, t^{-4} pulse profile gain more than 80% of the maximum possible energy gain of 3.3 eV. Generally, this mechanism for ion acceleration is found to be robust, causing substantial acceleration over a wide range of experimental parameters.

The effects discussed in this article likely dominate the energy spectrum of positive ions emitted from a pulsed-laser-irradiated conductive surfaces at low laser fluence. It follows that the experimental observation of ions with several volts of energy does not require the existence of an energetic surface emission process. These results are applicable to the low-laser-power limit where ablation of surface material can

be ignored. We find that the potency of this ion acceleration mechanism diminishes only logarithmically with peak laser intensity.

ACKNOWLEDGMENTS

This research was supported by the Northwest College and University Association for Science (Washington State University) under Grant No. DE-FG06-89ER-75522 and by the Division of Chemical Sciences, Office of the Basic Energy Sciences of the Department of Energy. Pacific Northwest Laboratory is operated by Battelle Memorial Institute for the Department of Energy under Contract No. DE-AC06-76RL0 1830.

[1] J. C. Brand and S. M. George, Surf. Sci. **167**, 341 (1986).
[2] S. A. Buntin, L. J. Richter, D. S. King, and R. R. Cavanagh, J. Chem. Phys. **91**, 6429 (1989).
[3] A. de Meijere, H. Hirayama, and E. Hasselbrink, Phys. Rev. Lett. **70**, 1147 (1993).
[4] E. P. Marsh, T. L. Gilton, W. Meier, M. R. Schneider, and J. P. Cowin, Phys. Rev. Lett. **61**, 2725 (1988).
[5] E. P. Marsh, F. L. Tabare, M. R. Schneider, T. L. Gilton, W. Meier, and J. P. Cowin, J. Chem. Phys. **92**, 2004 (1990).
[6] S. J. Dixon, E. T. Jensen, and J. C. Polanyi, Phys. Rev. Lett. **67**, 2395 (1991).
[7] V. A. Ukraintsev, T. J. Long, T. Gowl, and I. Harrison, J. Chem. Phys. **96**, 9114 (1992).
[8] M. von Allmen, *Laser-Beam Interactions with Materials* (Springer, Berlin, 1987).
[9] E. van de Riet, J. C. S. Kools, and J. Dieleman, J. Appl. Phys. **73**, 8290 (1993), and references therein.
[10] *Laser Ablation, Mechanisms and Applications*, edited by J. C. Miller and R. F. Haglund (Springer, Berlin, 1991).
[11] J. C. S. Kools, S. H. Brongersma, E. van de Riet, and J. Dieleman, Appl. Phys. B **53**, 125 (1991).
[12] P. G. Strupp, P. C. Stair, and E. Weitz, J. Appl. Phys. **69**, 3472 (1991).
[13] R. W. Dreyfus, J. Appl. Phys. **69**, 1721 (1991).
[14] T. M. Orlando, J. P. Cowin, G. Teeter, and S. E. Barlow, in *Laser Ablation: Mechanisms and Applications—II*, AIP Vol. 288 (AIP, New York, 1993), p. 341.
[15] T. L. Gilton, J. P. Cowin, G. D. Kubiak, and A. V. Hamza, J. Appl. Phys. **68**, 4802 (1990).
[16] V. P. Ageev, V. I. Konov, and A. I. Krechetov, Sov. J. Quantum Electron. **20**, 949 (1990).
[17] K. R. Spangenberg, *Vacuum Tubes* (McGraw-Hill, New York, 1948), Chap. 8.
[18] E. A. Berchenko, A. V. Koshkin, A. P. Sobolev, and B. T. Fedyushin, Sov. J. Quantum Electron. **8**, 1582 (1981).
[19] C. R. Phipps, T. P. Turner, R. F. Harrison, G. W. York, W. Z. Osborne, G. K. Anderson, X. F. Corlis, L. C. Haynes, H. S. Steele, K. C. Spicochi, and T. R. King, J. Appl. Phys. **64**, 1083 (1988).
[20] W. L. Smith, Opt. Eng. **17**, 489 (1978).
[21] R. C. Davidson, *Physics of Nonneutral Plasmas* (Addison-Wesley, Redwood City, CA, 1990).
[22] D. Nicholson, *Plasma Theory* (Wiley, New York, 1983), p. 5.
[23] D. Nicholson, *Plasma Theory* (Wiley, New York, 1983), p. 14.
[24] C.-L. Wang, G. Joyce, and D. R. Nicholson, J. Plasma Phys. **25**, 225 (1981).